A Calibration Technique for Radioactive Gas Monitor with a Built-in Germanium Detector

M. Yoshida[1], T. Oishi[1], J. Saegusa[1], T. Honda[2], K. Takahashi[3] and H. Kuwabara[4]
[1] Japan Atomic Energy Research Institute, Tokai, Ibaraki, Japan
[2] Institute of Radiation Measurement, Tokai, Ibaraki, Japan
[3] SEIKO EG&G Co., Ltd., Takatsuka, Matsudo, Chiba, Japan
[4] Hitachi, Ltd., Omika, Hitachi, Ibaraki, Japan

1. INTRODUCTION

Various types of radioactive gas monitors are utilized for evaluation of the radioactive gases released from nuclear facilities(1). Most of them are fabricated with gas-flow ionization chamber or plastic scintillation counter for beta-ray emitters, and NaI(T*l*) scintillation counter for gamma-ray emitters. It is not easy to make them accurately evaluate the activity for each radioactive nuclide because of their radiation detection mechanism or poor gamma-ray peak resolution. In these days, therefore, the gas monitor based on gamma-ray spectrometry with germanium detectors (hereinafter Ge gas monitor) has been developed for identification of the released radioactive nuclides(2). In order to measure the activity for each radioactive nuclide using the Ge gas monitors, it is important to determine the peak-detection efficiency curve vs. gamma-ray energy for gaseous sources in a sampling vessel.

The calibration of gas monitors, in general, should be carried out with radioactive standard gases. However, the number of radioactive gases available for calibration is not so many. The whole peak-detection efficiency curve over the gamma-ray energy range of interest should be obtained by proper interpolation of those limited data.

This paper describes the calibration technique for the Ge gas monitor with several radioactive gases, and a traditional calibration technique based on interpolation of the measured data with a multi-gamma-ray point source. The results of calibration with radioactive gases are discussed in comparison with those obtained by the experiments with the point source. The feasibility of interpolation based on a Monte Carlo simulation is also discussed.

2. EXPERIMENTS AND CALCULATION

2.1 Determination of detection efficiency with radioactive gases

The Ge gas monitor calibrated in the present work consists of a germanium detector and a Marinelli-shaped sampling vessel, as shown in Fig. 1. The outer shell of sampling vessel, made of polyvinyl chloride (PVC), is 241 mm in inner diameter, 250 mm in inner height and 3 mm thick. The cylindrical part containing the germanium detector head is 96 mm in diameter and 135 mm in height. It is also made of PVC and its wall is 3 mm thick. The germanium detectors combined with the sampling vessel are of closed end type, whose relative efficiencies are nominally 10% and 25%.

The closed gas loop used for calibration of the Ge gas monitor is shown in Fig. 2, which comprises a gas standard instrument, a mixing pump, a pressure gauge, a carrier gas inlet and exhaust lines. For the gas standard instrument, a gas-flow ionization chamber with an effective volume of 1500 cm^3 was used. Its ionization current was measured with a vibrating-reed electrometer. The response of the ionization camber was evaluated on the basis of absolute radioactivity measurements by Length Compensation method(3) and Diffusion-in Long Proportional Counter method(4). The uncertainty of the radioactivity concentration determined by the ionization chamber is less than 4% for each radioactive gas in dry air.

The radioactive gases of ^{133}Xe, ^{135}Xe, ^{85}Kr and ^{41}Ar were applied for the calibration(5). Among them, the short half-lived gases of ^{133}Xe, ^{135}Xe and ^{41}Ar were produced by (n, γ) reaction in a thermal neutron field of JAERI research reactor. The available gamma-ray energy, emission rate, half-life and impurity of the produced gases are given in Table 1.

On the calibration of the Ge gas monitor, after uniformly circulating the mixture of radioactive gases and dry air through the closed gas loop, the detection efficiency of built-in germanium detector was determined from the radioactivity concentration inside the loop and the count rate in a full-energy peak area of gamma-ray energy spectrum. The full-energy peak area was analyzed by SEIKO EG&G Gamma Studio system.

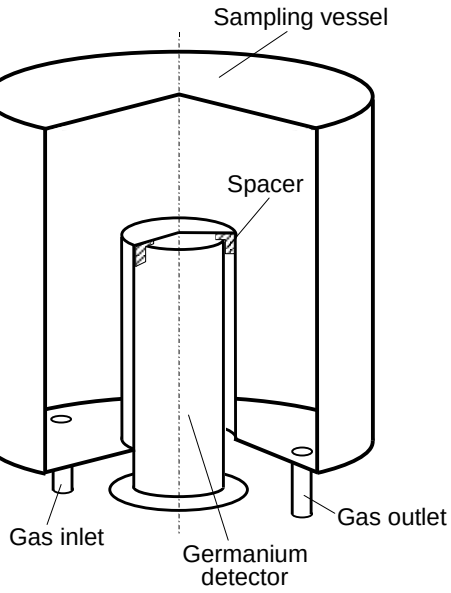

Fig. 1 Cutaway view of the sampling vessel of Ge gas monitor.

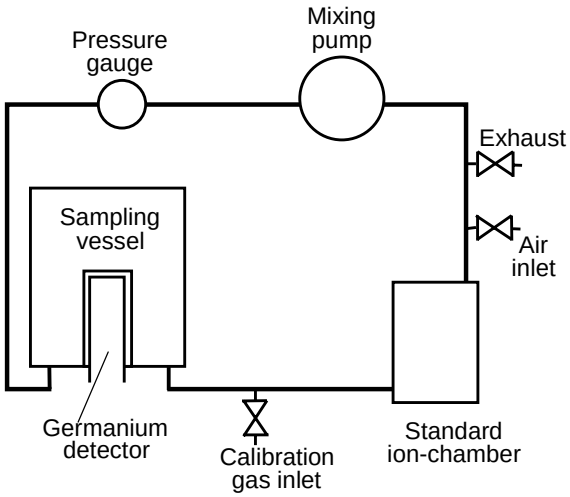

Fig. 2 Closed gas loop for calibration of the Ge gas monitor with radioactive gases.

Table 1 Half-life, Gamma-ray energy, emission rate and impurity of calibration gases.

Nuclide	Half-life	Gamma-ray energy - keV - (Emission rate)	Impurity - % -
^{133}Xe	5.24 d	81.0 (38.3)	< 1.5
^{135}Xe	9.14 h	249.8 (90.2)	< 0.1
		608.2 (2.90)	---
^{85}Kr	10.8 y	514.0 (0.43)	< 0.1
^{41}Ar	1.82 h	1293.6 (99.1)	< 0.1

2.2 Determination of detection efficiency with multi-gamma point source

The germanium detector was also calibrated with a multi-gamma source which was purchased from AEA Technology in UK. The source has a plastic layer incorporated with 10 radioactive nuclides, 10 mm in diameter and 0.2 mm thick. The dimension of the source can be approximately regarded as a point source in this experiment although it is not of real point. The nuclides delivered into the source, their activities and the available gamma-ray energies for the determination of detection efficiency curves are listed in Table 2. The overall uncertainty of radioactivity is 3 % in a confidence level of approximately 95 %.

The experimental system was set up in a shielding box with a lead wall of 100 mm in thickness. The measurement was made for 112 points at intervals of 2 cm on a plane including the detector axis, as shown in Fig. 3. The detection efficiency curve was determined for each position in the same manner of gamma-ray spectrum analysis as for the gaseous radioactivity measurements.

Table 2 Nuclides contained in the point source, activity and available gamma-ray energy.

Contained nuclide	Activity (kBq)	Gamma-ray energy(keV)
^{241}Am	3.4	60
^{109}Cd	16.4	88
^{57}Co	0.6	122
^{139}Ce	0.6	166
^{203}Hg	0.6	279
^{113}Sn	2.0	392
^{85}Sr	1.6	514
^{137}Cs	3.2	662
^{60}Co	3.5	1173
		1333
^{88}Y	4.0	898
		1836

Over all uncertainty is less than 3(%).

2.3 Estimation of detection efficiency by calculation

The detection efficiency of the built-in germanium detector was calculated by Monte Carlo simulation codes of EGS-4(6) and MCNP4B(7). In depiction of the germanium detector for the calculation, were precisely taken into consideration the dimensions of germanium crystal, lithium contact dead layer, electrode, end cap and other structures, as shown in Fig. 4. Gamma-ray sources were postulated to uniformly distribute in the air inside the sampling vessel. The detection efficiency was defined as a ratio of the number of the events in which the whole energy deposited in the germanium crystal to that of the generated gamma rays. The calculation for each gamma-ray energy was executed until the fractional standard deviation in its full-energy peak became less than 0.05. The cutoff energies for secondary gamma rays and electrons are 10 keV.

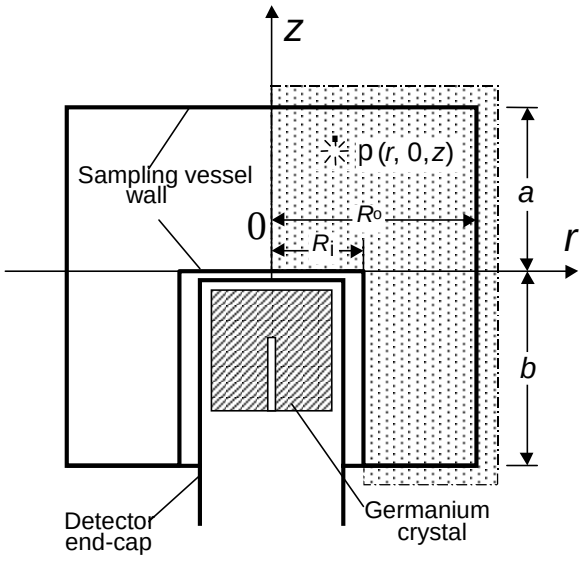

Fig. 3 Layout of a point source for estimation of the detection efficiency curve. P (r, 0, z) is any position on a plane including the detector axis. The point source was located inside the dotted area.

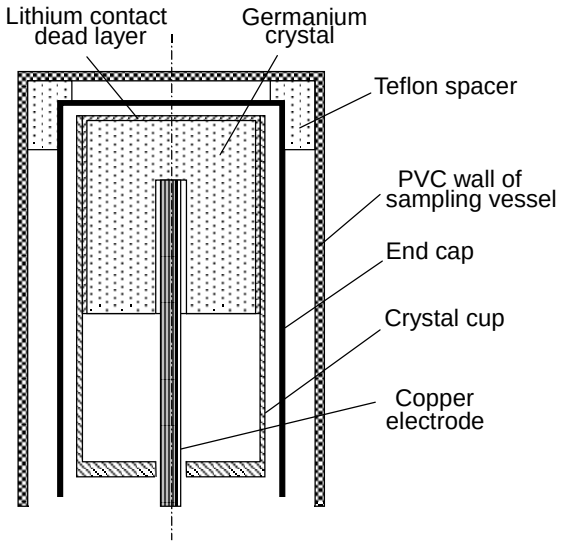

Fig. 4 Structure of the well part of sampling vessel and the germanium detector, applied for Monte Carlo simulation.

3. RESULTS AND DISCUSSION

Table 3 gives the detection efficiencies of the Ge gas monitor, which were determined with the four gaseous radioactive nuclides. The overall uncertainty of the efficiency in this calibration is less than 8 % in a confidence level of approximately 95%. It includes the uncertainties concerning the handling of radioactive gases in the loop, the measurement of radioactivity concentration with the standard ionization chamber, the determination of the peak area in gamma-ray spectrum, etc.

Table 3 Resultant detection efficiencies determined with gaseous sources.

Nuclide	Gamma-ray energy (keV)	Detection efficiency	
	10%-Ge	25%-Ge	
^{133}Xe	81.0	(4.18±0.30)E-3	(4.95±0.35)E-3
^{135}Xe	249.8	(5.26±0.33)E-3	(8.49±0.53)E-3
	608.2	(1.90±0.13)E-3	(3.76±0.26)E-3
^{85}Kr	514.0	(2.55±0.18)E-3	(4.52±0.32)E-3
^{41}Ar	1293.6	(1.08±0.07)E-3	(2.25±0.15)E-3

In the case of radioactive gases uniformly distributing over within the sampling vessel, the detection efficiency, η, can be derived on the basis of the detection efficiency for a point source at each position with the following equation.

$$\eta = 2\{\int_0^a \int_0^{R_o} F(r,z)\cdot r\cdot drdz + \int_{-b}^0 \int_{R_i}^{R_o} F(r,z)\cdot r\cdot drdz\} \Big/ \left\{aR_o{}^2 + b\left(R_o{}^2 - R_i{}^2\right)\right\} \qquad (1)$$

Where $F(r, z)$ is the detection efficiency for a point source located at the position (r, 0, z) and can be obtained by Spline-interpolation of the efficiency-data matrix measured with the multi-gamma point source. The radii, R_o and R_i, and the heights, a and b, are defined in Fig. 3.

The resultant efficiency curves derived from equation (1) and with the data matrices for the point source are shown in Fig. 5, accompanying the results for gaseous sources given in Table 3. Two curves correspond to the germanium detectors of 10% and 25% in nominal relative efficiency, respectively. The measured points for the gaseous sources closely scatter along the curves within their uncertainties. This consistency confirms high reliability of each calibration method. The whole range of gamma-ray energy of interest can be covered by the method with the point source, even if there is a shortage of the number of calibration gas.

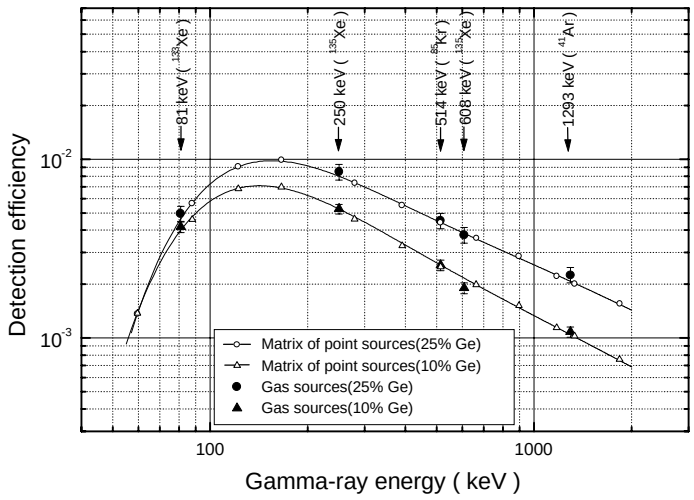

Fig. 5 Comparison of detection efficiency between with gaseous sources and from matrix of point source.

The typical position, where a point source gives as a similar detection efficiency curve as gaseous sources, can be determined from the data matrices measured with the point source. The position is determined from the minimal value of $s(r, z)$ with the following equation.

$$s(r,z) = (1/n)\sum_{i=1}^{n} \left\{1 - F_{E_i}(r,z)/\eta_{E_i}\right\}^2 \qquad (2)$$

Where $F_{Ei}(r, z)$ and η_{Ei} are the $F(r, z)$ and η, which are described in equation (1), for a gamma-ray energy of E_i, respectively, and n is the number of gamma-ray energy point.

The distribution of $s(r, z)$ for the 10% germanium detector is shown as a contour map in Fig. 6. Three minimal positions of P1, P2 and P3 are observed in the contour map. As seen in Fig. 7, the efficiency curves corresponding to the minimal positions are consistent each other. Especially the efficiency curve at the position of P3 shows good agreement within the error of 3% with that given by equation (1). The quite similar results were obtained for the 25% germanium detector. This agreement suggests that the calibration with a reference point source placed at the position enables easy and accurate determination of the efficiency for this type of gas monitors.

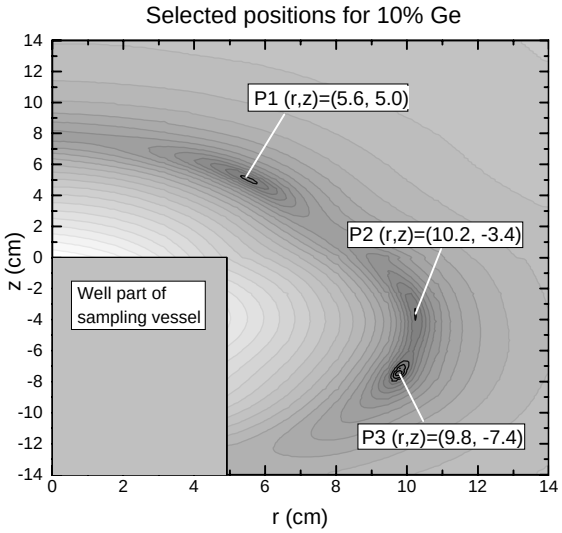

Fig. 6 Contour map showing three selected positions, the efficiency curves for which are the closest to the curve estimated for the whole volume of sampling vessel.

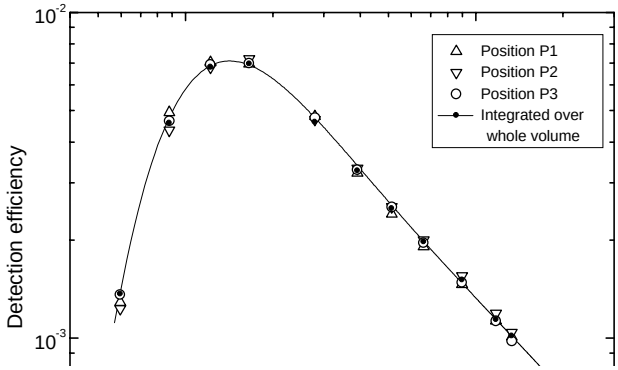

Fig. 7 Detection efficiency curves corresponding to three selected positions for the 10% germanium detector. The symbols, △,▽and○, shows the positions of P1, P2 and P3, respectively.

Figure 8 shows the efficiency curves for the 10% germanium detector calculated by a Monte Carlo code of MCNP-4B. The results by the code and another code of EGS-4 gave consistent curves within the error of each calculation. Thickness of the lithium contact dead layer is postulated to be 0.7 mm for the curve (a) in Fig. 8, according to the specification of the detector. The efficiency at a gamma-ray energy of 662 keV on the curve (a) is about 25% larger than the corresponding measured one. The difference is much larger in the lower energy part of the curve. Even in the curve (b), where the thickness of dead layer is 1.5 mm, the efficiency is not consistent well with the measured one. Hence, it is difficult to apply the calculated efficiency curves to interpolation of the measured points with gaseous sources.

The effective volume of germanium detector does not coincide with the whole volume of germanium crystal, because regions of insufficient charge collection can exist in the crystal as well as surface dead layer. More detailed depiction of the structure of germanium detector, including inside the crystal, must be required to explain the measured values precisely. However, since the calculation can easily give the distribution of detection efficiency instead of the data matrices measured with the point source, it might be useful for selecting the minimal position as mentioned above.

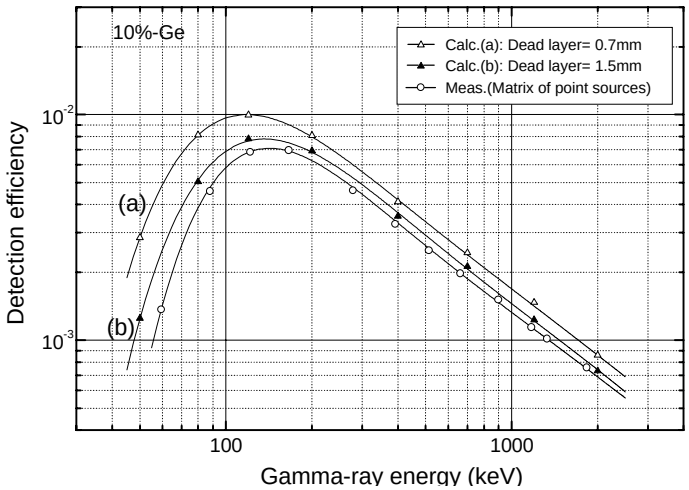

Fig. 8 Comparison of the detection efficiency curves calculated with MCNP-4B to that obtained with the measured point-source data. The resultant curves are shown only for the 10% germanium detector. In the calculation, the dead layers are assumed to be (a)0.7 mm and (b)1.5 mm thick.

4. CONCLUSION

The calibration with radioactive gases was carried out to determine the response of the Ge gas monitor, reflecting its real measurement conditions. The detection efficiencies of the monitor were determined for five energies corresponding to the gamma rays emitted from four gaseous radioactive nuclides. On the other hand, they were estimated on the basis of the data matrices of efficiency measured with a multi-gamma ray point source. Both the measured results of efficiency with the gaseous sources and the point source show good agreement within their uncertainties. According to both results, the reliable detection efficiency curve can be obtained over the whole gamma-ray energy range of interest.

The positions around the germanium detector, where a point source gives as similar detection efficiency curve as gaseous sources, were searched from distribution of the deviation of the efficiency. As a result, it was found out that one of the closest efficiency curves gave agreement within an error of 3%. This method leads to easy and accurate calibration for this type of gas monitor, substituting the complicated calibration method with gaseous sources.

The efficiencies calculated with the Monte Carlo simulation code were somewhat larger than the measured ones. The discrepancy is considered to depend on insufficient depiction of the structure inside the germanium crystal for the code. More detailed information about the surface dead layer and region of bad charge collection in the crystal must be required in order to apply the simulation for determining absolute detection efficiencies.

REFERENCES

1. International Electrotechnical Commission, *Equipment for continuously monitoring radioactivity in gaseous effluents Part 3: Specific requirements for noble gas effluent monitors*, Publication 761-3 (1983).
2. L. Erbeszkorn, Á. Szörényi and J. Vágvölgyi, Nucl. Instrum. Methods A369, 463-466 (1996).
3. S. B. Garfinkel, W. B. Mann, F. J. Schima and M. P. Unterweger, Nucl. Instrum. Methods 112, 59-67(1973).
4. C. Mori, T. Yamamoto, T. Suzuki, A. Uritani, K. Yanagida, Y. Wu, T. Watanabe and M. Yoshida, Nucl. Instrum. Methods. A312, 189-192 (1992).
5. M. Yoshida, T. Oishi, T. Honda and T. Torii, Nucl. Instrum. Methods A383, 441-446 (1996).
6. W. R. Nelson, SLAC-265 (1985).
7. J. F. Briesmeister (Ed), LA-12625-M (1997).